Supporting Information

Constructing Rigid–Flexible Robust Silicone Aerogels via Hyperconnected POSS Networks for Extreme Thermal Protection

Aoqing Yan, [a, b] *Guixiang Li,* [b, *] *Yi Luo,* [b, *] *Bing Han,* [a] *Zhe Su,* [b] *Hao Tian,* [a]

Bo Niu [a] *and Donghui Long* [a, b, *]

[a] Key Laboratory of Specially Functional Polymeric Materials and Related Technology (Ministry of Education), School of Chemical Engineering, East China University of Science and Technology, Shanghai 200237, China.

[b] Suzhou National Laboratory, No.388, Ruoshui Street, SIP, Jiangsu 215123, China

* Corresponding author: longdh@mail.ecust.edu.cn (D.H. Long), liguixiang1998@163.com (G.F. Li), and sosolyi@163.com (Y. Luo)

Part A: Detailed information of ablation test

Here, the size of ablation specimen was Φ30 × 10 mm. The tests were performed with 5 parallel specimens to ensure statistical significance. A K-type thermocouple was utilized to record thermal responses on the backside surfaces. The linear ablation rate (R_l) and mass ablation rate (R_m) were calculated by employing the following formulas:

$$R_l = (l_0 - l_t)/t \qquad \text{* MERGEFORMAT (1)}$$

$$R_m = (m_0 - m_t)/t \qquad \text{* MERGEFORMAT (2)}$$

Where l_0 and m_0 represents the thickness and mass before ablation, l_t and m_t represents the thickness and mass after ablation, and t is the ablation time.[1]

Part B: Supplementary Figures and Tables

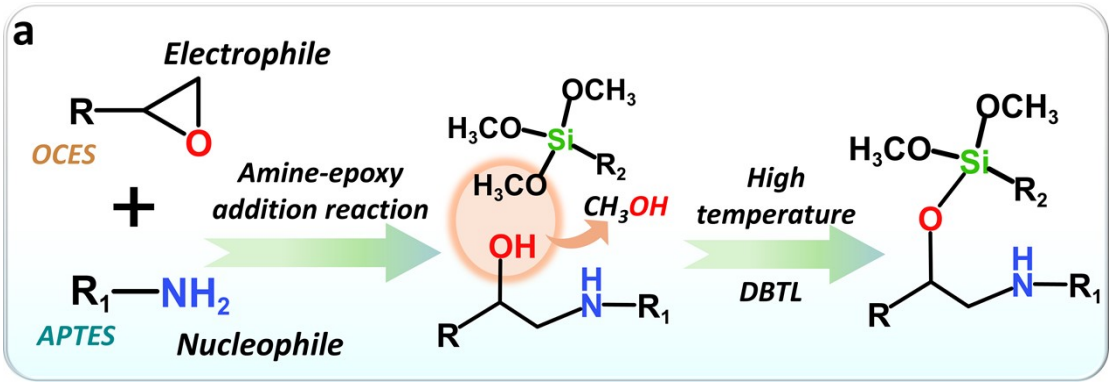

Fig. S1 Schematic of the synthesis route for POSS-SAE.

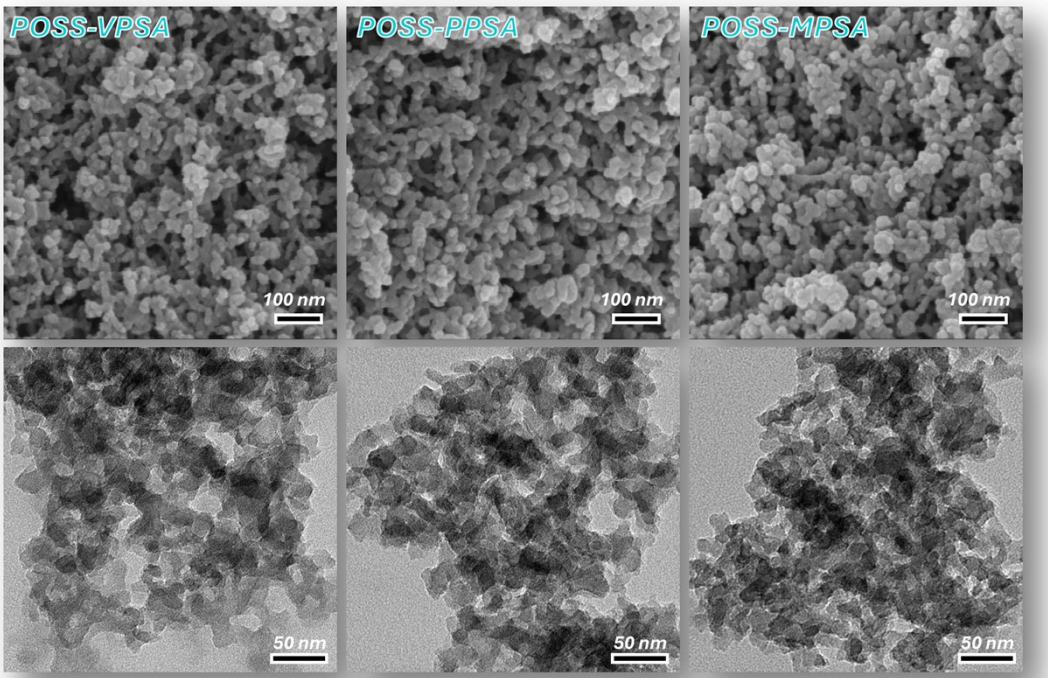

Fig. S2 SEM and TEM images of POSS-PSAs.

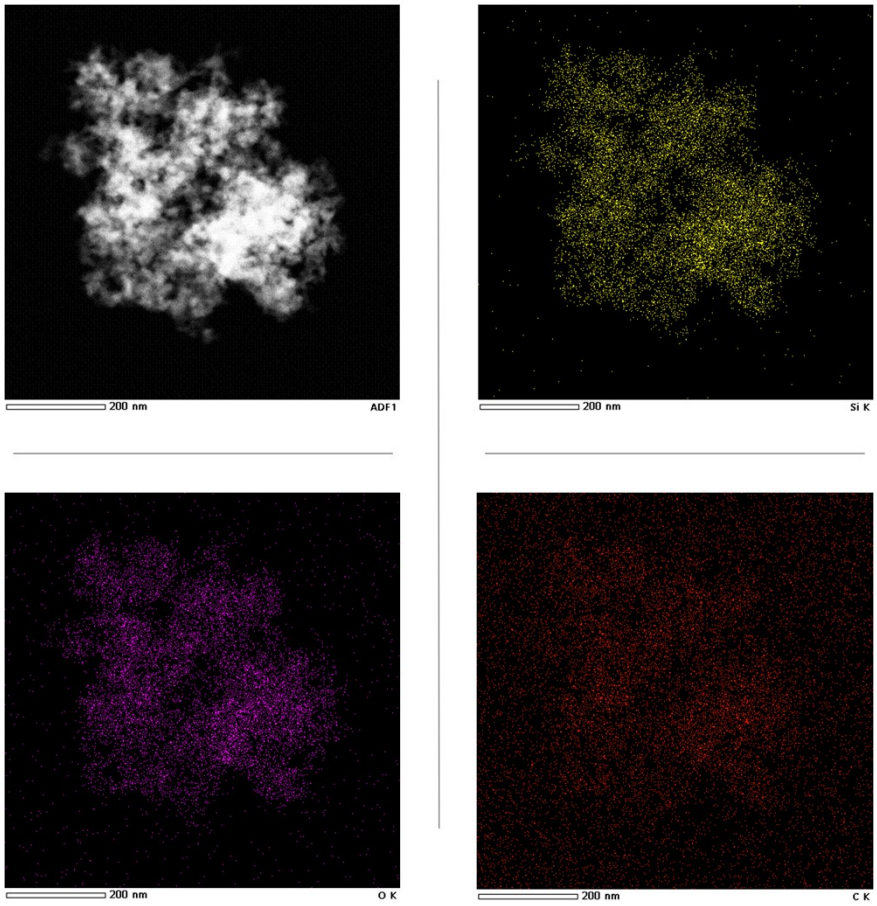

Fig. S3 Elemental mapping of POSS-VPSA.

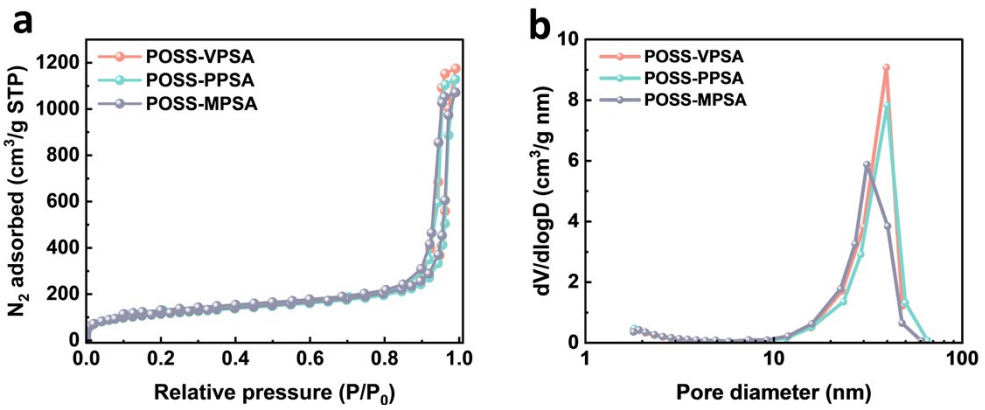

Fig. S4 BET Analysis Results of the POSS-PSAs. (a) N_2 adsorption/desorption isotherms. (b) Pore size distribution.

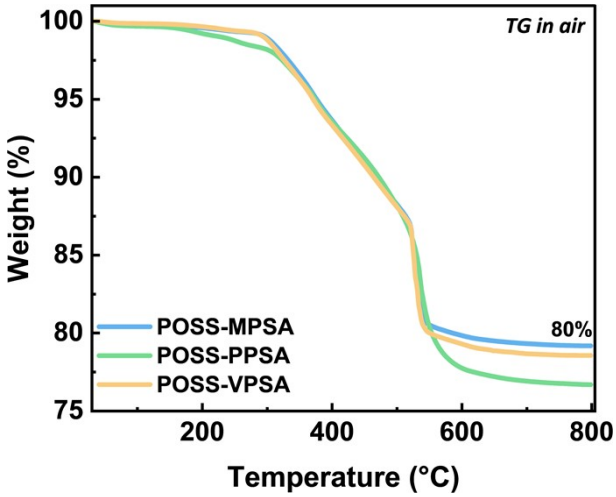

Fig. S5 TG curves of POSS-PSAs under air atmosphere.

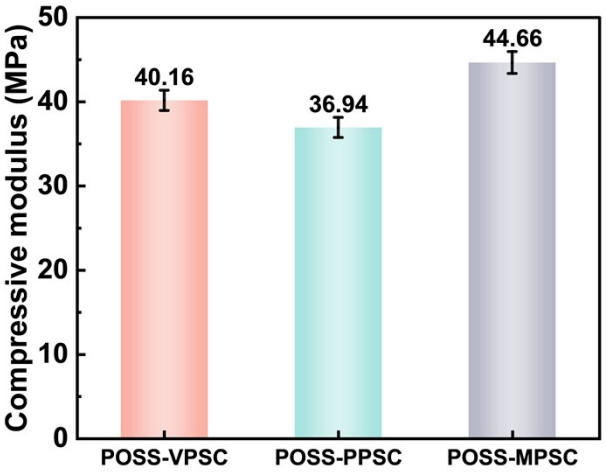

Fig. S6 Compressive modulus of POSS-PSCs.

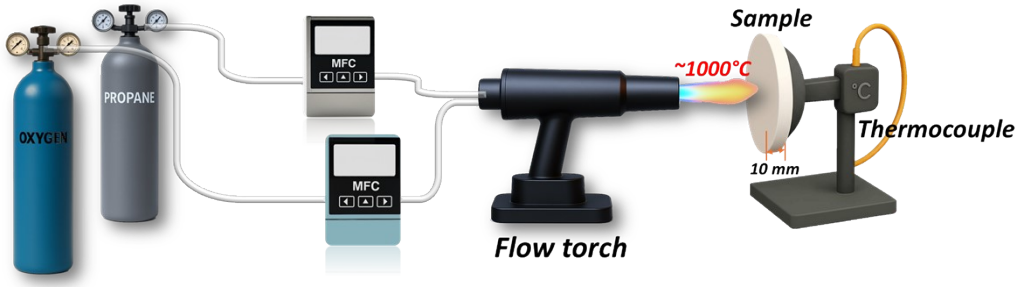

Fig. S7 Schematic diagram of oxy-propane ablation system.

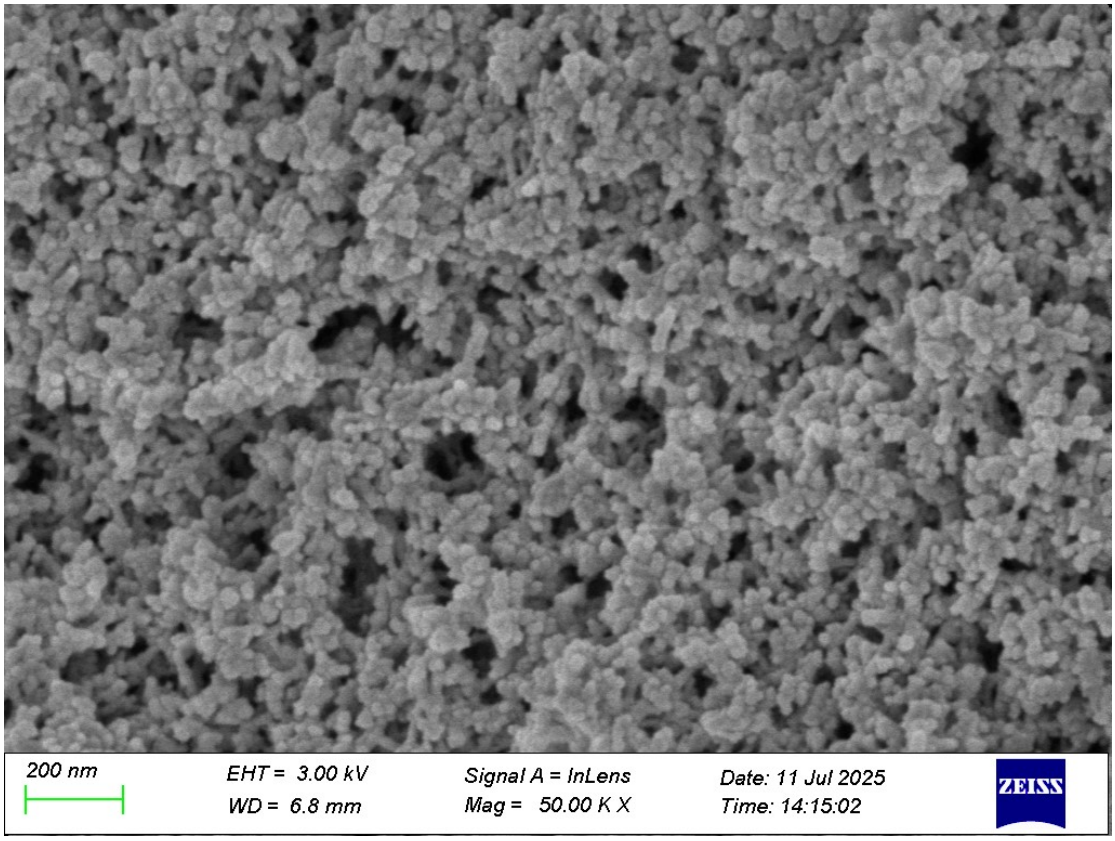

Fig. S8 SEM image of POSS-VPSC after the oxygen–propane flame ablation at 1000 °C.

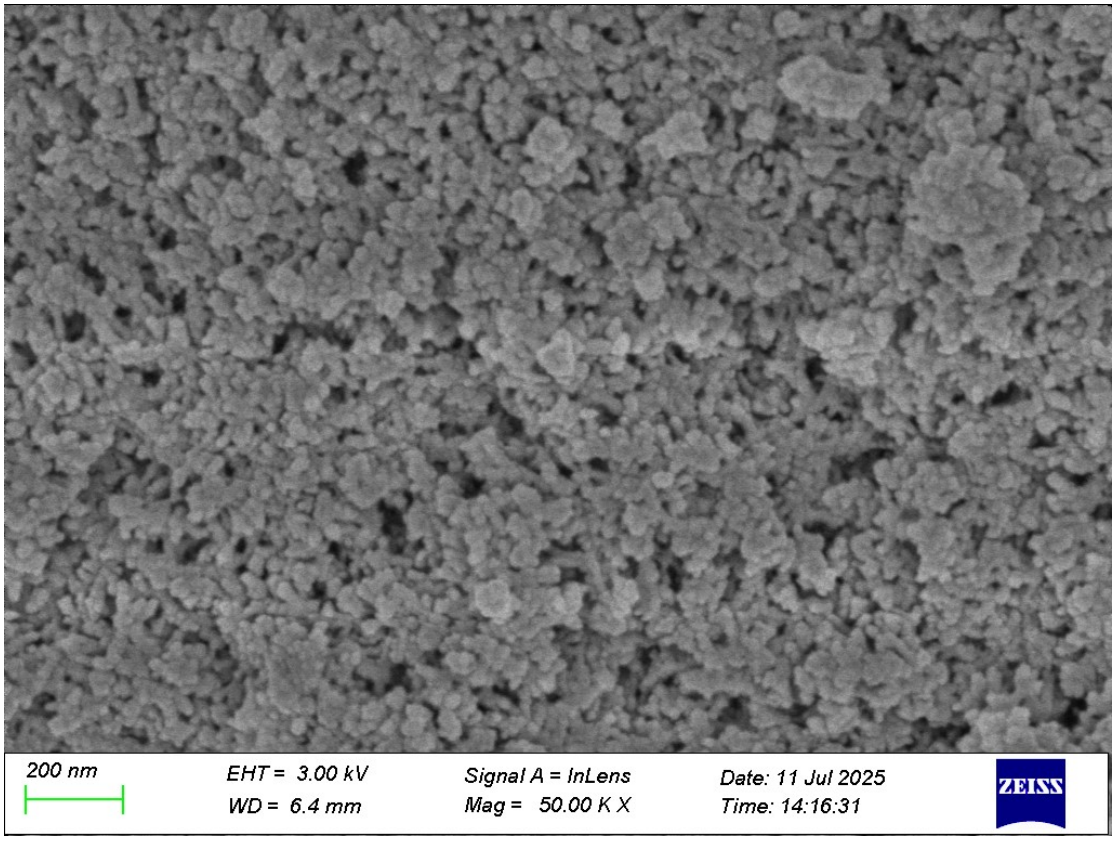

Fig. S9 SEM image of POSS-VPSC after the oxygen–propane flame ablation at 1400 °C.

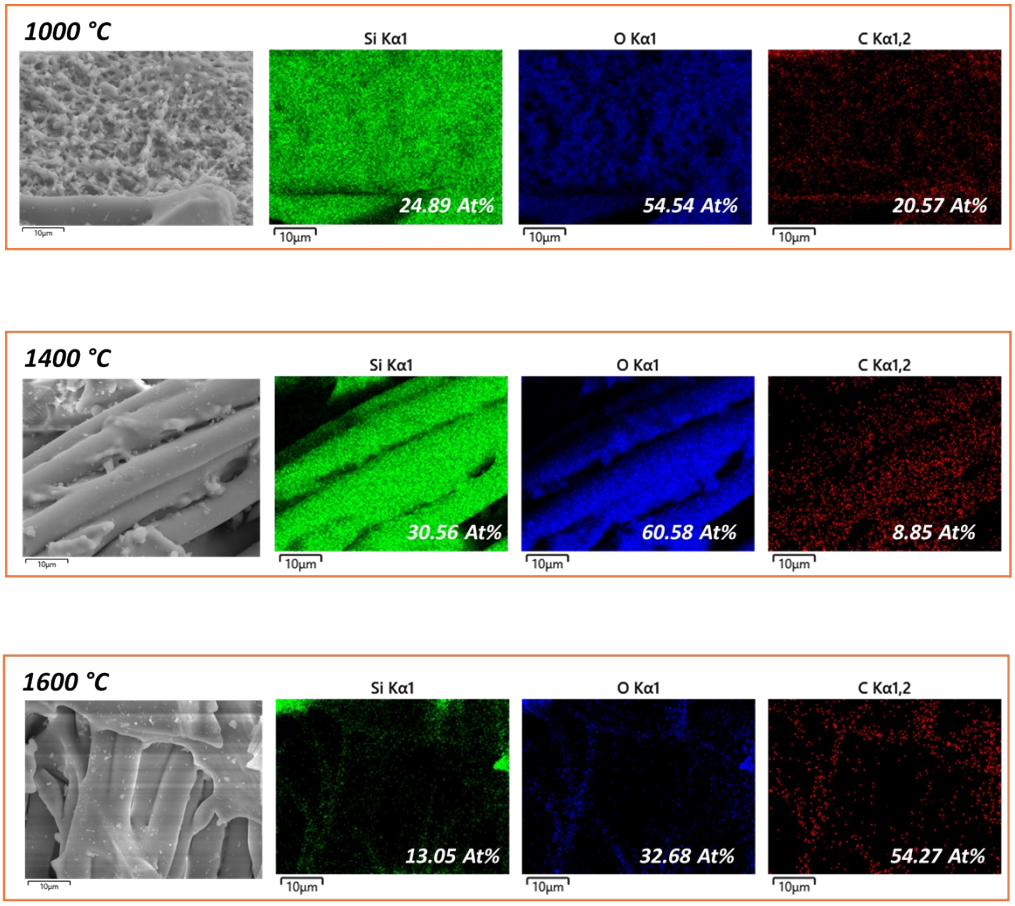

Fig. S10 SEM image and EDS elemental mappings of the POSS-VPSC composite surface after ablation at different temperatures.

Table S1. Amount of Deionized Water for POSS-PSA Preparation with Various POSS-SAEs

POSS-SAE	Deionized Water (g)
POSS-VSAE	0.61
POSS-PSAE	0.56
POSS-MSAE	0.63

Table S2. Typical physical properties of the aerogels

Sample	Bulk density ($g \cdot cm^{-3}$)	Volume shrinkage (%)	Mean pore diameter [a] (nm)	S_{BET} [b] (m^2/g)	Pore volume (cm^3/g)	λ [c] ($W \cdot m^{-1} \cdot K^{-1}$)
POSS-VPSA	0.35	5	18.8	413	1.80	0.036
POSS-PPSA	0.34	4	19.5	412	1.72	0.035
POSS-MPSA	0.37	8	17.6	421	1.64	0.038

[a]Mean pore diameter obtained from nitrogen adsorption branch via the Barrett−Joyner−Halenda method. [b]Brunauer−Emmett−Teller SSA obtained from nitrogen adsorption measurement. [c]Thermal conductivity at room temperature and ambient pressure.

Table S3. Typical physical properties of the composites

Sample	Bulk density (g/cm^3)	Volume shrinkage (%)	Compressive modulus (MPa)	λ [c] ($W \cdot m^{-1} \cdot K^{-1}$)
POSS-VPSC	0.50	3	55.5	0.037
POSS-PPSC	0.49	2	52.8	0.036
POSS-MPSC	0.52	5	58.4	0.038

Table S4 Detailed comparison of mechanical and thermal properties of various aerogels (corresponding to Fig. 4g)

Sample	Bulk density (g/cm^3)	Compressive Strength (MPa)	Thermal Conductivity ($W \cdot m^{-1} \cdot K^{-1}$)	Test Conditions	Ref.
POSS-MPSA	0.37	6.10	0.038	RT[a]	This Work
MK/SiO_2 aerogel	0.29	3.24	0.031	RT[a]	2
PMMS/PMDMS silicone aerogel	0.42	5.83	0.052	RT[a]	3
SiO_2NWs-reinforced silica aerogel	~0.12	~1.38[b]	0.037	RT[a]	4
Chitosan/silica hybrid aerogel	0.17	~0.24[c]	0.028	RT[a]	5

a Room temperature; b Compressive stress recorded at 60% strain; c Compressive stress recorded at 5% strain

Table S5 Detailed comparison of mechanical and thermal properties of various composites (corresponding to Fig. 5e)

Sample	Fiber Content (wt%)	Bulk density (g/cm^3)	Tensile Strength (MPa)	Thermal Conductivity ($W \cdot m^{-1} \cdot K^{-1}$)	Test Conditions	Ref.
POSS-MPSC	38.5	0.52	27.8	0.038	RT[a]	This Work
Silicone/ Quartz fiber composites	40.0	0.50	15.5	0.039	RT[a]	6
Silicone/fibrous ceramic tile	66.7	0.45	3.6	0.06	RT[a]	7
Fiber-reinforced alumina–silica aerogel composites	38.5	0.39	1.8	0.039	RT[a]	8
Silicone/phenolic/ quartz/carbon hybrid fiber	57.6	0.33	16.8	0.062	RT[a]	9
SiO_2/quartz fiber	48.3	0.58	4.3	0.042	RT[a]	10

a Room temperature

Reference

1 H. Cai, B. Niu, Z. Qian, T. Li, P. Wang, L. Li, Y. Cao, Y. Zhang and D. Long, *Composites Science and Technology*, 2024, **245**, 110325.

2 L. Xu, W. Zhu, Z. Chen and D. Su, *ACS Appl. Mater. Interfaces*, 2023, **15**, 44238–44247.

3 Y. Luo, A. Yan, H. Tian, B. Niu, Y. Zhang, H. Wang and D. Long, *J. Mater. Chem.A*, 2024, **12**, 4684–4694.

4 L. Wang, W. Lian, B. Yin, X. Liu and S. Tang, *Ceram. Int.*, 2024, **50**, 6693–6702.

5 S. Zhang, Y. Liao, K. Lu, Z. Wang, J. Wang, L. Lai, W. Xin, Y. Xiao, S. Xiong and F. Ding, *Carbohydr. Polym.*, 2023, **320**, 121245.

6 H. Tian, Y. Luo, Z. Su, A. Yan, X. Liang, Y. Xing, B. Niu and D. Long, *Compos. Part A-appl. S.*, 2025, **198**, 109107.

7 H. Tian, X. Dong, B. Niu, Z. Su, A. Yan, X. Liang, Y. Xing, Y. Luo and D. Long, *Chem. Eng. J.*, 2025, 169346.

8 F. Peng, Y. Jiang, J. Feng, H. Cai, J. Feng and L. Li, *Chem. Eng. J.*, 2021, **411**, 128402.

9 X. Jin, C. Wu, H. Wang, Y. Pan, H. Huang, W. Wang, J. Fan, X. Yan, C. Hong and X. Zhang, *Compos. Sci. Technol.*, 2023, **232**, 109878.

10 K. Xu, C. Wu, Z. Chen, H. Liu, M. Li, L. Yang, S. Ai and S. Cui, *Ceram. Int.*, 2025, **51**, 2094–2103.